



UNIVERSITY OF LEEDS

This is a repository copy of *Phosphate and ammonium sorption capacity of biochar and hydrochar from different wastes.*

White Rose Research Online URL for this paper:
<http://eprints.whiterose.ac.uk/93527/>

Version: Accepted Version

Article:

Takaya, CA, Fletcher, LA, Singh, S et al. (2 more authors) (2016) Phosphate and ammonium sorption capacity of biochar and hydrochar from different wastes. *Chemosphere*, 145. pp. 518-527. ISSN 0045-6535

<https://doi.org/10.1016/j.chemosphere.2015.11.052>

© 2015, Elsevier. Licensed under the Creative Commons Attribution-NonCommercial-NoDerivatives 4.0 International
<http://creativecommons.org/licenses/by-nc-nd/4.0/>

Reuse

Unless indicated otherwise, fulltext items are protected by copyright with all rights reserved. The copyright exception in section 29 of the Copyright, Designs and Patents Act 1988 allows the making of a single copy solely for the purpose of non-commercial research or private study within the limits of fair dealing. The publisher or other rights-holder may allow further reproduction and re-use of this version - refer to the White Rose Research Online record for this item. Where records identify the publisher as the copyright holder, users can verify any specific terms of use on the publisher's website.

Takedown

If you consider content in White Rose Research Online to be in breach of UK law, please notify us by emailing eprints@whiterose.ac.uk including the URL of the record and the reason for the withdrawal request.



eprints@whiterose.ac.uk
<https://eprints.whiterose.ac.uk/>

1 Phosphate and ammonium sorption capacity of biochar and hydrochar from 2 different wastes

3 C.A. Takaya¹, L.A. Fletcher², S. Singh¹, K.U. Anyikude¹, A. B. Ross^{1*}

4 ¹Energy Research Institute, School of Chemical and Process Engineering,
5 University of Leeds; ²School of Civil Engineering, University of Leeds,
6 LS2 9JT, United Kingdom.

7 *Corresponding Author: A.B.Ross@leeds.ac.uk; Tel: +44(0) 113 3431017

8 9 **Highlights**

- 10 • PO₄-P adsorption capacity is more dependent on char calcium and
11 magnesium content than on other ash components.
- 12 • NH₄-N adsorption capacity is a function of oxygen-containing functional
13 groups, and physisorption is not the dominant mechanism for NH₄-N
14 adsorption.
- 15 • Similarities in char sorption capacities regardless of processing conditions and
16 feedstock.

17 18 **Abstract**

19 The potential for biochar and hydrochar to adsorb phosphate and ammonium is
20 important for understanding the influence of these materials when added to soils,
21 compost or other high nutrient containing environments. The influence of
22 physicochemical properties such as mineral content, surface functionality, pH and
23 cation exchange capacity has been investigated for a range of biochars and

24 hydrochars produced from waste-derived biomass feedstocks. Hydrochars produced
25 from hydrothermal carbonisation at 250 °C have been compared to low and high
26 temperature pyrolysis chars produced at 400-450 °C and 600-650 °C respectively for
27 oak wood, presscake from anaerobic digestate (AD), treated municipal waste and
28 greenhouse waste. In spite of differences in char physicochemical properties and
29 processing conditions, PO₄-P and NH₄-N sorption capacities ranged from about 0-30
30 mg g⁻¹ and 105.8-146.4 mg g⁻¹ respectively. Chars with high surface areas did not
31 possess better ammonium adsorption capacities than low surface area chars, which
32 suggests that surface area is not the most important factor influencing char
33 ammonium adsorption capacity, while char calcium and magnesium contents may
34 influence phosphate adsorption. Desorption experiments only released a small
35 fraction of adsorbed ammonium or phosphate (< 5 mg g⁻¹ and a maximum of 8.5 mg
36 g⁻¹ respectively).

37 Keywords: Waste; Phosphate and Ammonium adsorption; Biochar; Hydrochar.

38

39 **1. Introduction**

40 Phosphate and ammonium recovery is important from an environmental
41 management aspect as these species are contributors to eutrophication (Rittmann et
42 al. 2011; Wang et al. 2015a; Zeng et al. 2013) and can be found in several
43 wastewaters at varying concentrations (Bott et al. 2000; Barker et al. 2001; Battistoni
44 et al. 2006; Cai et al. 2013; Grzmil and Wronkowski 2006; Song et al. 2011; Liu
45 2009; Ye et al. 2010). Ammonium makes up a very high proportion of soluble
46 nitrogen in animal waste and can be adsorbed onto negatively-charged sites or
47 between clay interlayers in soils (Fernando et al. 2005). When released however,

48 nitrifying bacteria convert this to nitrate in aerobic conditions which is eventually
49 leached to groundwater (Fernando et al. 2005). Phosphate recovery is also
50 important because an essential plant nutrient, there are growing concerns about its
51 future availability (Rittmann et al. 2011). A number of ammonium and phosphate
52 adsorbents have therefore been considered including chars obtained from the
53 thermal treatment of organic matter in an oxygen-free atmosphere (biochars) or in
54 the presence of subcritical water (hydrochars). Both biochars and hydrochars are
55 heterogeneous structures comprised of carbonized organic matter, inorganic matter,
56 sorbed volatiles and functional groups of nitrogen, sulphur and oxygen (Knicker
57 2007; Spokas et al. 2012). They are becoming increasingly attractive in a number of
58 sectors as they can be derived from a wide range of waste biomass feedstocks and
59 show potential as cost-effective, environmentally sustainable products for integrated
60 waste management. Indeed, the application of biochars as adsorbents for soil
61 nutrients, wastewater contaminants, pathogens and gases have been widely
62 researched (Collison et al. 2009; Laird et al., 2010a; Spokas et al. 2012a; Wang et
63 al. 2015a; Zeng et al. 2013; Zheng et al. 2010).

64 While several studies have highlighted positive, neutral and in some cases negative
65 responses to biochar applications in a number of soils (Biederman and Harpole
66 2013; Spokas et al. 2012a; Uzoma et al. 2011), the mechanism by which chars
67 adsorb nutrients and thus enhance soil productivity is not fully understood owing to
68 variations in climate and soil. Furthermore, as char properties are a function of the
69 nature of feedstocks used and biomass processing conditions (Collison et al. 2009;
70 Wang et al. 2015a; Zhao et al. 2013), these variations further contribute to the
71 challenges involved with quantifying their effect on nutrient cycling. Moreover,
72 biochars influence nutrient cycling via biological, physical and chemical processes in

73 the short- and long-term (Laird et al. 2010a; Biederman and Harpole 2013). In the
74 short-term, labile fractions of biochar and hydrochar may introduce bioavailable
75 phosphorus and potassium to soils (Biederman and Harpole 2013; Laird et al.
76 2010b; Uzoma et al. 2011) as well as retain nutrient-rich soil water within their pores,
77 while long-term biochar effects could involve creating favourable habitats for soil
78 fungi such as mycorrhizae which influence nutrient cycling (Yamato et al. 2006).
79 Chars may also increase soil alkalinity, resulting in an increase in phosphorus
80 availability since at acidic conditions ($\text{pH} < 4$), this nutrient would be bound as
81 insoluble iron and aluminium phosphates by aluminium and iron oxides respectively
82 (Biederman and Harpole 2013; Uzoma et al. 2011; Xu et al. 2014). Char Cation
83 Exchange Capacity (CEC) and surface chemistry could also influence nutrient
84 retention (Laird et al. 2010a; Silber et al. 2010; Wang et al. 2015b); for instance,
85 Zheng et al. (2010) observed that surface chemistry (negative surface charge) and
86 metal-phosphate precipitation reactions played a more important role than surface
87 area in the ammonium and phosphate sorption capacities respectively. Indeed,
88 Borchard et al. (2012) noted that only specific types of biochars can improve soil
89 nutrient retention, aggregation and CEC, and that these biochars tend to possess
90 hydrophilic surfaces. It is hypothesised that biochar produced at lower temperatures
91 may have better ammonium adsorption capacity due to the presence of increased
92 negatively-charged functional groups like carboxylates (Liang et al. 2006), and a
93 positive relationship has been observed between biochar CEC, surface area and
94 ammonium sorption (Zeng et al. 2013). Conversely, biochar phosphate adsorption
95 capacity is thought to increase with increasing levels of metal ions, thus biochars
96 with lower ash content will have lower phosphate adsorption capacities.

97 The objectives of this work were therefore to: (i) investigate the potential for
98 phosphate and ammonium recovery by biochars and hydrochars produced from
99 various feedstocks; (ii) investigate the influence of physicochemical properties
100 including elemental content, mineral content and surface functionality on nutrient
101 sorption and adsorption mechanisms. Overall, this work was aimed at promoting a
102 better understanding of the interaction of nutrients with biochars and hydrochars and
103 how this may impact their application.

104

105 **2. Methods**

106 **2.1 Materials**

107 A set of five feedstock have been used in this study: oak wood and greenhouse
108 waste sourced from Andalucia, Spain; Anaerobically Digested (AD) waste sourced
109 from Organic Waste Systems (OWS), Belgium; treated municipal waste sourced
110 from Graphite resources, UK. Chemicals for various analyses were used as
111 received.

112 **2.2 Biochar and hydrochar production**

113 Samples of biochar were produced by Energy research Centre of the Netherlands
114 (ECN) at 400 °C and 600 °C using a screw thread Pyromaat reactor. Pyrolysis chars
115 were also supplied by a commercial pyrolysis plant operated by Proiniso, Spain.
116 Hydrochars were produced at the University of Leeds using a 500 mL stainless steel
117 Parr 4836 reactor. Hydrothermal Carbonization (HTC) experiments were performed
118 using 10 wt. % solids/water slurries at 250 °C for 1 h at approximately 4 MPa
119 following which the hydrochars were filtered and air-dried.

120 **2.3 Biochar and hydrochar characterisation**

121 2.3.1 Agronomical analyses

122 Ultimate analyses of biochar and hydrochar samples were determined using a CHN
123 Elemental Analyser (Thermo Scientific Flash 2000). Proximate analysis was
124 performed in a muffle furnace following the BS method for biomass. Macro- and
125 micro-nutrient content of the chars was determined after acid digestion of chars in
126 concentrated nitric acid and analyzed by Inductively-coupled Plasma-Mass
127 Spectroscopy (Perkin Elmer) following digestion in nitric acid. pH measurements
128 were made after 1:20 char/distilled water mixtures were shaken and allowed to stand
129 for 2 h. Solvent extraction of chars was performed by exhaustive soxhlet extraction
130 at room temperature using toluene. Solid state NMR has been performed in cross-
131 polarisation mode on a Bruker Avance III HD for chars from Oak wood by
132 hydrothermal carbonisation at 250 °C and pyrolysis at 400 °C and 600 °C. This facility
133 is operated by the University of Durham, EPSRC facility.

134 CEC was determined using a method similar to that of Brewer (2012), Gaskin et al.
135 (2008) and Yuan et al. (2011). 20 mL distilled water was added to 1g of biochar and
136 shaken at 160 rpm for 10 minutes each in a water shaker bath (SW23 Julabo GmbH)
137 at room temperature and filtered through a Whatman Grade 1 filter paper. This was
138 repeated four more times, discarding the leachates each time. Biochars were
139 saturated with 10 mL of 1M sodium acetate (Alfa Aesar) with pH adjusted to 7 using
140 a few drops of glacial acetic acid, shaken at 160 rpm for 16 minutes and filtered. This
141 was repeated twice more, discarding the leachates each time, after which biochars
142 were rinsed with ethanol (Fischer Scientific UK) thrice for 8 minutes each at 160 rpm.
143 Three additions of 1 M ammonium acetate (Fischer Scientific UK) at pH 7 were used
144 to displace sodium cations by shaking at 160 rpm for 16 minutes, storing the

145 leachates for subsequent analysis. Analyses were done in duplicate or triplicate, and
146 the average values are reported. The concentration of displaced sodium cations
147 were determined by Atomic Absorption Spectroscopy (AAS) of 10 mL aliquots of the
148 final leachates.

149 **2.4 Phosphate and ammonium adsorption capacity**

150 2.4.1 Batch adsorption

151 All containers were acid washed with 1 M HCl and rinsed with deionised water
152 before use. 0.1 g biochar ($\leq 850 \mu\text{m}$) was transferred to plastic Nalgene containers
153 and 100 mL of 125 mg P L^{-1} phosphate solution prepared from potassium phosphate
154 monobasic (Fischer Scientific UK) was added after its pH was adjusted to 7 with 1 M
155 NaOH. The containers were tightly sealed and shaken at 160 rpm for 24 h in a water
156 shaker bath (SW23 Julabo GmbH) at room temperature. 10mL aliquots of each
157 sample were taken after 24 h and filtered through $0.45 \mu\text{m}$ Sartorius Minisart syringe
158 filters for Ion Chromatography analysis (Metrohm 850 Professional IC–AnCat). This
159 procedure was repeated for ammonium solutions, using about $1000 \text{ mg NH}_4^+\text{-L}^{-1}$
160 prepared from ammonium chloride (Fischer Scientific UK). Most analyses were done
161 in duplicate and the average values reported. The concentrations of adsorbed ions
162 were determined as:

$$163 \quad q_e = (C_o - C_e) \frac{V}{M} \quad (1)$$

164 where C_o and C_e = initial and equilibrium liquid-phase phosphate or
165 ammonium adsorbate concentrations respectively (mg L^{-1}); V = volume of
166 solution (L); M = mass of char (g).

167

168 2.4.2 Desorption isotherms

169 Adsorbed phosphate and ammonium in chars were extracted using a similar
170 procedure as outlined above but using 0.01 M KCl solution. 10 mL aliquots of each
171 sample were taken after 24 h then filtered through 0.45 μm Sartorius Minisart syringe
172 filters for Ion Chromatography analysis.

173 2.4.3 Adsorption kinetics

174 To investigate possible phosphate and ammonium adsorption mechanisms, 0.1 g
175 chars ($\leq 850\mu\text{m}$) were each added to 125 mg P L⁻¹ or 1000 mg NH₄⁺ L⁻¹ solutions
176 respectively, as done in **Section 2.4.1** but 10 mL aliquots of each sample were taken
177 at 2.5, 5, 7.5, 10 and 24 h. Samples were filtered, analysed by Ion Chromatography
178 and the concentration of adsorbed ions were determined.

179 2.4.4 Adsorption isotherms at varying initial concentrations

180 0.1 g of char with highest carbon contents (oak and greenhouse waste) was added
181 to varying concentrations of phosphate solutions, specifically 50-200 mg P L⁻¹, and
182 ammonium concentrations ranging from about 360-815 mg NH₄⁺ L⁻¹. These
183 concentrations were chosen to represent some real-case wastewater concentrations.
184 The mixtures were shaken at 160 rpm for 24 h at room temperature, keeping all
185 other parameters identical to batch adsorption tests. Samples were filtered, analysed
186 by Ion Chromatography and the concentration of adsorbed ions were determined as
187 in **Section 2.4.1**.

188

189

190 **3. Results and Discussion**

191 **3.1 Effect of pyrolysis on biochar physicochemical properties**

192 As pyrolysis temperature increases, carbon content predictably increases as shown
193 in **Table 1**. Volatile matter was generally higher in hydrochars while ash contents
194 were comparable in both hydro- and bio-chars. Oak chars generally had lower ash
195 contents compared to waste chars, which is likely why carbon contents in the former
196 were higher; wood chars are known to possess higher cellulose and hemicellulose
197 contents which carbonize during pyrolysis (Kizito et al. 2015). Biochar pH values
198 were alkaline, ranging from 8.6-11.1 while hydrochars were mostly acidic, ranging
199 from 4.8-7.2. In accordance with European Biochar Certificate requirements for
200 biochars intended for soil amendment (IBI 2014), carbon contents were > 50% dry
201 mass for greenhouse waste chars and both oak chars, O/C ratios were < 0.4 in all
202 chars except 400°C municipal waste biochar and H/C ratios were < 0.7 in all but 4
203 chars (hydrochars of presscake, greenhouse waste, municipal waste and 400°C
204 municipal waste biochars). Both oak wood samples exhibited similar
205 physicochemical characteristics, both possessing the highest carbon contents.
206 Calcium and magnesium contents were generally higher than the other macro-
207 minerals (**Table 2**); the former ranged from 1.6-8.1% and increased with pyrolysis
208 temperature while magnesium contents ranged from 0-1.2%, with most biochars
209 possessing 0.2-0.5%.

210

211

212

213 3.2 Biochar and hydrochar CEC

214 CEC is known to decrease with an increase in pyrolysis temperature (Lehmann
215 2007; Silber et al. 2010), but only non-commercial oak chars (OW) exhibited this
216 trend (**Table 2**). Higher temperature biochars (600-650 °C) generally had higher CEC
217 than lower temperature biochars (400-450 °C). Regardless of their higher oxygen
218 contents, hydrochar CEC values were generally lower than biochar CEC, however,
219 positive correlations between bio- and hydro-char oxygen content and CEC were
220 found ($\rho_{X,Y} = 0.8$) as expected (Wang et al. 2015b). No relationship between char
221 CEC and surface area was evident; for instance, the CEC of 450 °C commercial oak
222 and 400 °C presscake biochars were similar despite marked differences in surface
223 area ($180 \text{ m}^2 \text{ g}^{-1}$ and $2 \text{ m}^2 \text{ g}^{-1}$ respectively). The results indicate that oak and
224 greenhouse waste typically produce a higher CEC than the municipal waste and
225 presscake biochars possibly because these feedstocks contain higher lignocellulosic
226 contents and lower ash contents.

227 To better understand the CEC trends, CEC measurements were performed on chars
228 following solvent extraction in toluene compared with as-received chars. Solvent
229 extraction had different effects on the two types of char: in hydrochars, the CEC in
230 most cases improved (**Fig. 1(a)**); in biochars, the CEC remained unchanged or
231 decreased after solvent extraction, the latter more prevalent for the higher
232 temperature biochars (**Fig. 1(c)**). As CEC is said to be a function of surface area and
233 functionality, an increase in hydrochar CEC following solvent extraction could
234 suggest either the unblocking of pores increasing porosity and surface area, or that a
235 higher surface functionality is being revealed by removing tars. The latter effect may
236 be more important as surface area had negligible influence on char CEC, with
237 hydrochars possessing low surface areas ($< 6 \text{ m}^2 \text{ g}^{-1}$). Based on the assumption that

238 carboxyl and other functional groups improve CEC (Boehm 1994; Glaser et al. 2002;
 239 Warner 1977), the removal of volatile hydrocarbons from the surface of the biochar
 240 containing these groups by solvent extraction is expected to affect CEC by revealing
 241 a different surface functionality below.

242

Table 1. Char physicochemical properties

Biochar	C (%)	H (%)	N (%)	O [†] (%)	Ash content (%)	Volatile matter (%)
250°C hydrochars						
Oak wood	67.9	6.5	1.4	18.8	6.2	6.2
Greenhouse waste	66.4	6.8	3.1	18.3	5.2	61.6
Municipal waste	45.2	6.0	2.0	8.6	38.0	42.8
Presscake from AD	22.8	2.0	0.9	4.5	69.8	20.7
400-450°C biochars						
Oak wood (commercial)	65.7	2.7	0.6	8.9	11.7	21.1
Oak wood	70.9	3.6	0.4	12.9	12.1	20.8
Greenhouse waste	59.0	2.9	1.2	9.6	27.0	25.0
Municipal waste	39.9	3.7	1.7	4.2	50.1	26.2
Presscake from AD	17.1	0.8	0.9	1.5	79.5	13.4
600-650°C biochars						
Oak wood (commercial)	76.5	1.4	0.8	7.0	14.3	11.8
Oak wood	79.2	2.0	0.3	3.5	13.4	9.2
Greenhouse waste	63.0	1.2	0.9	7.5	17.0	13.0
Municipal waste	40.1	1.1	1.4	3.2	53.8	18.7
Presscake from AD	18.5	0.5	0.6	0.0	83.4	7.6

[†]O content determined by difference.

243

244

245

Table 2. Char pH and mineral composition

Biochar	pH	CEC ($\text{cmol}_e \text{ kg}^{-1}$)	P	K	Ca	Mg	Na
250°C hydrochars							
Oak wood	4.8	88.3 ± 9.7	1000	0	23,000	0	0
Greenhouse waste	5.8	83.1 ± 19.4	2000	7000	16,000	2000	0
Municipal waste	6.2	44.5 ± 1.7	3000	9000	24,000	4000	0
Presscake from AD	7.2	62.6 ± 3.5	5000	2000	27,000	6000	300
400-450°C biochars							
Oak wood (commercial)	9.9	59.4 ± 8.1	2000	11,000	44,000	2000	1000
Oak wood	9.7	105.8 ± 12.1	1000	9000	27,000	2000	1000
Greenhouse waste	10.6	109.5 ± 21.8	4000	41,000	36,000	9000	4000
Municipal waste	9.5	65.7 ± 16.2	5000	9000	53,000	5000	8000
Presscake from AD	10.3	51.0 ± 5.5	6000	12000	39,000	6000	4000
600-650°C biochars							
Oak wood (commercial)	10.3	76.6 ± 0.7	2000	6000	50,000	3000	0
Oak wood	8.6	65.2 ± 20.2	1000	2000	3100	0	0
Greenhouse waste	11.0	146.2 ± 32.3	4000	50,000	45,000	12,000	4000
Municipal waste	10.2	67.9 ± 12.5	5000	9000	81,000	5000	14,000
Presscake from AD	10.1	52.6 ± 11.5	5000	11,000	36,000	5000	4000

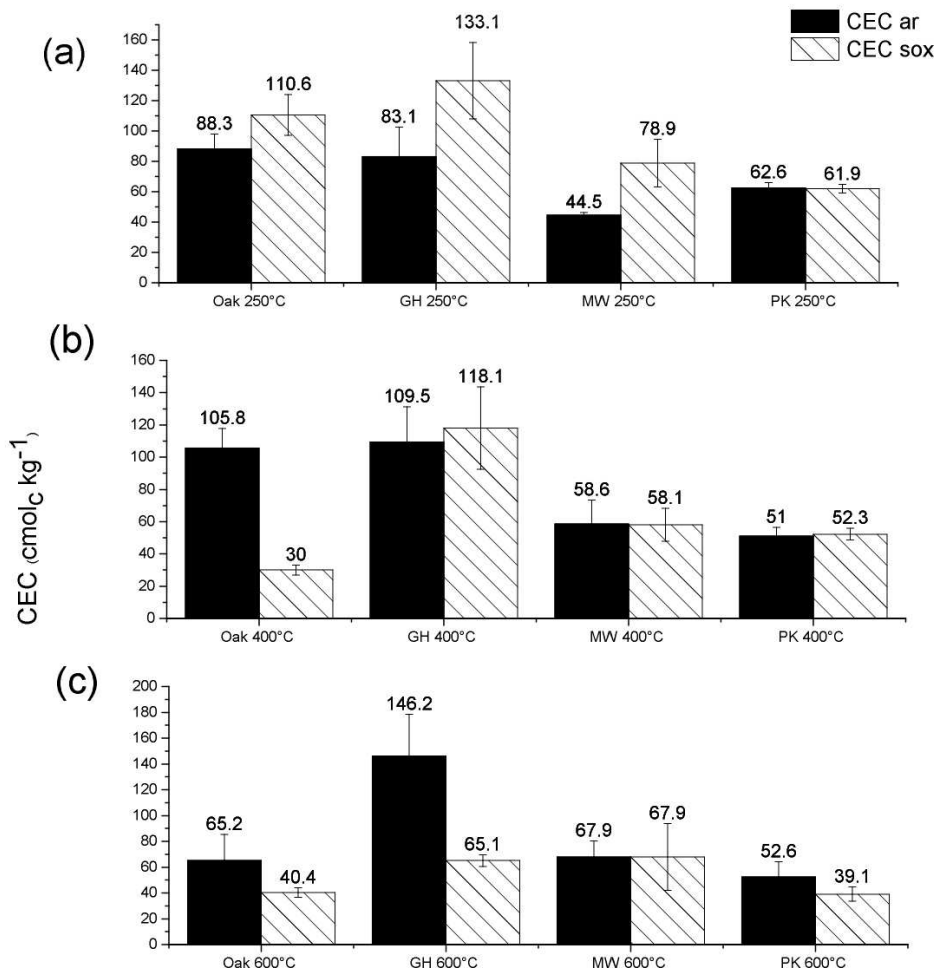
Mineral contents determined on dry basis (db) and reported in ppm.

246

247 Biochar CEC was generally similar before and after extraction but for the 600-650°C
 248 biochars, CEC was slightly higher for the as-received biochars indicating that solvent
 249 extraction reduced their surface functionality. There are some anomalies as
 250 observed in 400°C oak biochar, but the general emerging trend shows that
 251 hydrochar CEC is enhanced after extraction while biochars are either unaffected or
 252 lowered after extraction. This provides supporting evidence that CEC is potentially
 253 higher for hydrochar but the levels of tars on its surface affect its CEC. Indeed,
 254 water-insoluble fatty acids were found sorbed onto hydrochars produced from

255 microalgae (Heilmann et al. 2011) and brewer's spent grain (Poerschmann et al.
 256 2015), based on analyses with ether and chloroform/methanol solvents respectively.
 257 In this study, NMR analysis of chars confirmed that the surface functionality of low
 258 and high temperature chars differed considerably, with high temperature biochars
 259 possessing fewer functional groups (**Supplemental Fig. A1**). Extracts analysed by
 260 GC-MS also confirmed the removal of oxygenated groups and hydrocarbons from
 261 hydrochars and biochars respectively (data not included).

262



263

264

Figure 1. Effect of solvent extraction on biochar CEC
 MW: municipal waste; GH: greenhouse waste; PK: presscake
 CEC_{ar} and CEC_{sox} refer to CEC before and after solvent extraction respectively

265 3.3 Char PO₄-P adsorption

266 PO₄-P concentrations in various wastewaters can range from <14 mg L⁻¹ to over
267 15,000 mg L⁻¹ (Battistoni et al. 2006; Cai et al. 2013; Grzmil and Wronkowski 2006).
268 In this study, PO₄-P at initial concentrations of about 400 mg PO₄³⁻ L⁻¹ were used,
269 and char PO₄-P sorption capacities are presented in **Table 3**. Most results had
270 coefficients of variation <5% but greenhouse waste samples consistently showed
271 much higher percent variations, likely due to sample heterogeneity. PO₄-P release
272 occurred in greenhouse waste and presscake hydrochars and 450°C commercial
273 oak biochar, and such release has also been observed in low and high temperature
274 biochars elsewhere (Zeng et al. 2013). PO₄-P release does not appear to be due to
275 char P content, as water extraction of chars using a similar procedure as outlined in
276 **Section 2.4.1** showed that oak hydrochars and commercial oak biochars produced
277 at 450°C and 650°C respectively released 1.18±0.04, 0.554±0.003 and 1.19±0.03
278 mg g⁻¹ PO₄-P while greenhouse waste biochars produced at 400°C and 600°C
279 released 2.1±0.1 and 3.5±0.2 mg g⁻¹ PO₄-P respectively. On the other hand, char P
280 might not always be completely extractable with concentrated acid (Mukherjee and
281 Zimmerman 2013) or by water.

282 The PO₄-P adsorption capacities of oak and greenhouse waste chars were
283 compared at varying initial concentrations as shown in **Figs. 2(a)-(b)**. PO₄-P
284 adsorption improved with increasing initial concentration possibly due to higher
285 concentration gradients, resulting in better filling of reactive adsorption sites (Chen et
286 al. 2013; Krishnan and Haridas 2008; Wang et al. 2011; Xue et al. 2009). However,
287 Chen et al. (2013) and Wang et al. (2011) found that while phosphate adsorption
288 increased with initial concentration, adsorption efficiency (i.e. removal ratio)
289 decreased possibly because of fewer active adsorption sites available at higher initial

290 PO₄-P concentrations. This was also the case for chars in this study, with adsorption
291 efficiencies highest at 170 mg PO₄-P L⁻¹ in most cases. While pyrolysis temperature
292 and feedstock composition variation did not affect char adsorption capacity
293 substantially, hydrochars generally exhibited lower adsorption capacities.

294 Linearized Langmuir isotherm models did not fit the data for any of the chars and the
295 linearized Freundlich isotherm model described the adsorption mechanism slightly
296 better, based on *R*² values and a better agreement between experimental and
297 calculated *q*_e values. The Freundlich model is said to suit phosphate sorption better
298 because as adsorbents become saturated, adsorption affinity decreases
299 exponentially (Sakadevan and Bavor 1998) or because of precipitation reactions
300 (Zeng et al. 2013). Conversely, the Langmuir model fitted better than Freundlich
301 model in Wang et al. (2011) and Zeng et al. (2013), possibly resulting from the effect
302 of biochar P release (Zeng et al. 2013). In this study, adsorption intensity (*n*) > 1
303 suggested positive adsorption in oak biochars and 400 °C greenhouse waste
304 biochars.

305 Linearized Langmuir isotherm (Type II): $\frac{1}{q_e} = \left(\frac{1}{k_a q_m} \right) \frac{1}{C_e} + \frac{1}{q_m}$ (2)

306 Linearized Freundlich isotherm: $\log q_e = \log K_F + \frac{1}{n} \log C_e$ (3)

307 where *q*_e and *q*_m = amount of species adsorbed at equilibrium and saturated
308 monolayer adsorption respectively (mg g⁻¹), *C*_e = equilibrium concentration
309 (mg L⁻¹), *n* = adsorption intensity, *K*_a and *K*_F = Langmuir and Freundlich
310 constants respectively (Ho 2004; Kumar and Sivanesan 2007).

Table 3. Char PO₄-P and NH₄-N sorption capacity

Biochar	PO ₄ -P				NH ₄ -N				
	q _e (mg g ⁻¹)	% PO ₄ ³⁻ ads.	K _d	Desorbed (mg g ⁻¹)	q _e (mg g ⁻¹)	% NH ₄ -N ads.	K _d	Desorbed (mg g ⁻¹)	Desorbability
250°C hydrochars									
Oak wood	26.6 ± 10.3	6	0.07	n.d	109.7 ± 14.1	12	0.12	n.d	0
Greenhouse waste	-9.6 ± 7.6	0	-0.02	n.d	121.7 ± 0.3	13	0.13	4.8	0.03
Municipal waste	5.1 ± 3.8	1	0.01	n.d	146.4 ± 5.8	14	0.16	4.0	0.03
Presscake from AD	37.0 ± 7.1	9	0.10	n.d	129.0 ± 19.5	17	0.16	4.2	0.03
400-450°C biochars									
Oak wood (commercial)	-0.3 ± 6.1	0	-0.001	n.d	100.9 ± 3.4	9	0.11	5.0	0.05
Oak wood	5.5 ± 19.0	1	0.01	n.d	129.4 ± 34.8	13	0.11	5.0	0.05
Greenhouse waste	18.7 ± 1.9	4	0.05	n.d	118.2 ± 26.9	12	0.13	4.8	0.04
Municipal waste	11.9 ± 4.3	3	0.03	n.d	137.3 ± 0.6	13	0.15	3.0	0.02
Presscake from AD	7.8 ± 1.4	2	0.018	n.d	105.8 ± 11.5	9	0.11	4.0	0.04
600-650°C biochars									
Oak wood (commercial)	15.1 ± 5.9	4	0.04	n.d	114.4 ± 3.4	11	0.12	5.0	0.04
Oak wood	3.6 ± 6.1	1	0.01	n.d	123.5 ± 28.7	12	0.16	n.d	0
Greenhouse waste	9.1 ± 6.5	2	0.02	8.5	99.3 ± 28.5	10	0.11	n.d	0
Municipal waste	14.3 ± 0.6	4	0.04	n.d	128.3 ± 6.7	13	0.14	2.8	0.02
Presscake from AD	30.0 ± 24.9	7	0.08	n.d	136.2 ± 18.1	13	0.15	2.2	0.02
Phosphate C_o ≈ 400 mg L⁻¹; ammonium C_o ≈ 1000 mg L⁻¹; n.d: not detected; desorbability = ratio of NH₄-N desorbed to NH₄-N adsorbed.									

312 PO₄-P adsorption was highest a few hours after sorption tests began with the
313 exception of 600 °C greenhouse waste biochar (**Supplemental Fig. A2**). This is
314 contrary to other studies, which observed adsorption equilibrium concentrations after
315 24 h at room temperature (Wang et al. 2011; Zhang et al. 2012). This might be due
316 to the higher PO₄-P concentration used in this study. Oak char kinetics followed a
317 more predictable pattern than greenhouse waste biochars, and based on linear
318 regression analysis, the pseudo-second order model provided the best fit.

319 **3.4 Possible reaction mechanisms for biochar PO₄-P sorption**

320 PO₄-P sorption mechanisms are thought to be dependent on metal ion reactions
321 (precipitation, surface deposition), surface area and surface functionality (Wang et al.
322 2015a; Yao et al. 2013; Zeng et al. 2013). The influence of biochar surface area on
323 PO₄-P adsorption is unclear but some studies suggest that its influence may be
324 minor compared to adsorbent elemental composition. Wang et al. (2015a) for
325 instance found that the best performing biochars did not possess superior surface
326 areas compared to other biochars. Previous studies have also suggested that since
327 biochars tend to be negatively charged, surface functionality may not influence
328 phosphate sorption a great deal (Yao et al. 2011; Zeng et al. 2013).

329 In this study, PO₄-P sorption capacity increased with pyrolysis temperature, with the
330 exception of commercial oak and greenhouse waste biochars (**Fig. 3**). This is in
331 agreement with findings of Wang et al. (2015a) who observed an increase in PO₄-P
332 adsorption with pyrolysis temperature up to a certain point (500 °C). Generally, char
333 PO₄-P sorption capacities in this study were found to be lower than other
334 adsorbents, but some positive correlation between PO₄-P adsorption and Ca or Mg
335 contents were observed in hydrochars and biochars, and to a lesser degree with ash
336 content. Xue et al. (2009) also found that adsorbent chemical composition was most

337 influential, leading to simultaneous chemical precipitation and ligand exchange
338 between adsorbent and PO₄-P. Furthermore, Yao et al. (2011) compared biochars
339 produced from raw and from anaerobically digested sugar beet tailings and found
340 that PO₄-P adsorption capacities increased in the latter biochars possibly due to the
341 presence of surface MgO as this compound was absent in the former. Other cations
342 including Ca²⁺, Al³⁺ and La are known to improve phosphate adsorption as well
343 (Wang et al. 2015a; Xue et al. 2009; Yao et al. 2013; Zeng et al. 2013), particularly if
344 they are present as basic functional groups. Wang et al. (2015a) for instance
345 observed that biochar PO₄-P adsorption capacity was a function of ketones, pyrones
346 and chromens based on a positive correlation of these groups with PO₄-P removal
347 efficiency, although *R*² values of 0.73 suggested that these groups were not solely
348 responsible.

349 PO₄-P desorption from chars in this study was minimal, hence PO₄-P desorbability,
350 described by Xue et al. (2009) and Ye et al. (2006) as a ratio of desorbed phosphate
351 to total adsorbed phosphate, could not be determined in all but 2 biochars. Low PO₄-
352 P desorption might have been because PO₄-P ions were strongly bound to the chars
353 or because the extracting solution was inadequate. As easily desorbed phosphates
354 may be indicative of physical adsorption rather than chemical adsorption (Xue et al.
355 2009), the former might be more likely. Xue et al. (2009) and Ye et al. (2006) also
356 found that basic oxygen furnace slag and palygorskite adsorbents respectively did
357 not desorb a lot of phosphate regardless of initial phosphate concentration although
358 desorbability increased to some extent with an increase in amount of adsorbed
359 phosphate.

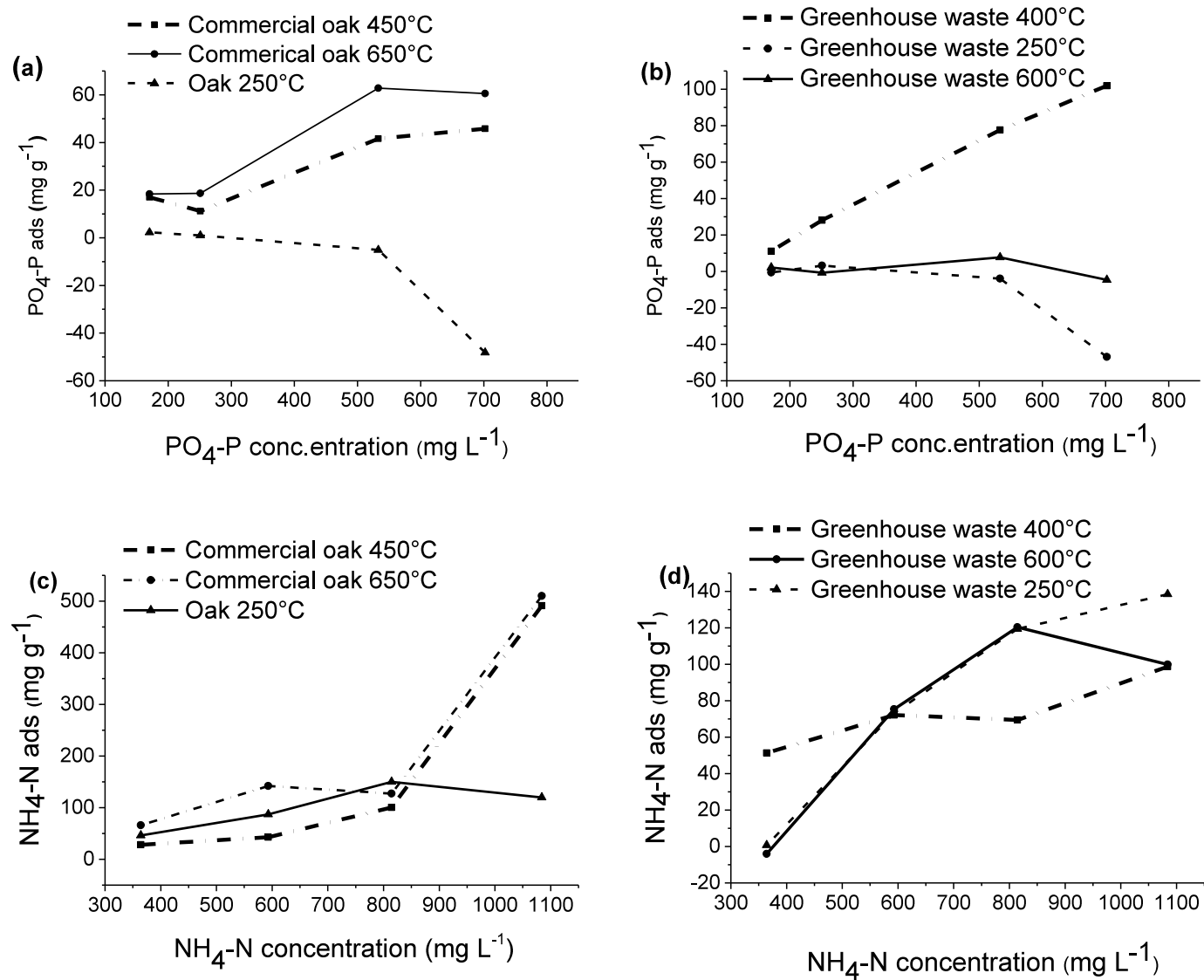


Figure 2. Effect of increasing PO₄-P and NH₄-N concentration on sorption on oak and greenhouse waste chars

361 Data fitted to kinetic models showed that the pseudo-second order model
362 consistently gave a closer fit compared to the pseudo-first order and intra-particle
363 diffusion models. While the latter two models gave average R^2 values of 0.53 and
364 0.28 respectively, the pseudo-second order R^2 values were higher (**Supplemental**
365 **Table A1**). Previous studies have also observed many metals and heavy elements
366 follow this pattern (Limousin et al. 2007). Wang et al. (2011) also found this model
367 fitted better than the intra-particle diffusion model. Based on their adsorption kinetics
368 data, simultaneous rapid surface adsorption of $\text{PO}_4\text{-P}$ and slower intra-particle
369 diffusion through the adsorbent occurred simultaneously.

370 Solvent extraction had variable effects on char $\text{PO}_4\text{-P}$ adsorption (**Fig. 3**). $\text{PO}_4\text{-P}$
371 adsorption improved in some low temperature biochars (400-450°C); 400°C oak
372 biochar which released phosphate into solution prior to extraction performed
373 marginally better after extraction. For 600-650°C biochars, solvent extraction
374 decreased % $\text{PO}_4\text{-P}$ adsorption however. These did not appear to be related to
375 volatile matter, ash content or elemental composition.

376

377

378

379

380

381

382

383

384

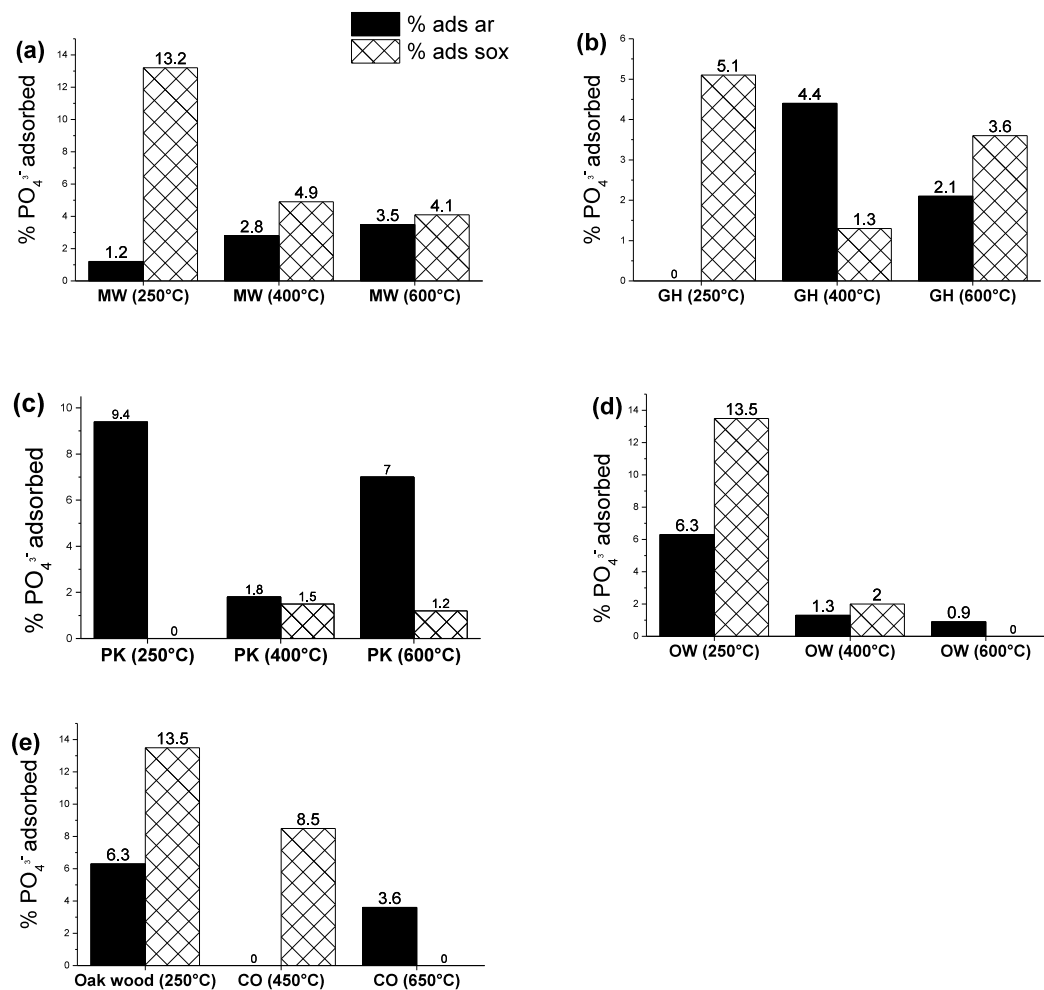


Figure 3. Comparison of $\text{PO}_4\text{-P}$ adsorption capacities of solvent extracted and non-extracted chars
PK: presscake; MW: municipal waste; CO: commercial oak; GH: greenhouse waste; OW: oak wood biochars solvent extracted chars are denoted 'sox'

385 3.5 Char NH₄-N sorption

386 Previous studies have shown that pH, time and initial NH₄⁺ concentrations are
387 important factors that determine biochar adsorption capacity (Fernando et al. 2005;
388 Kizito et al. 2015; Schlegel et al. 1999). NH₄-N adsorption increased at higher initial
389 solution concentrations but only to a certain point for oak hydrochar and 600°C
390 greenhouse waste biochar (**Figs. 2(c)-(d)**). Preliminary results showed that many
391 biochars released, rather than adsorbed NH₄-N at initial concentrations below 400
392 mg L⁻¹ (data not included). However, this may not be resulting from the lower initial
393 concentration since biochars are capable of adsorbing NH₄-N at low concentrations.
394 Subsequent adsorption tests with untreated biochars were however performed at a
395 higher initial concentration of about 1000 mg NH₄⁺ L⁻¹ and presented in **Table 3**.
396 NH₄-N adsorption data were fitted to the linearized Langmuir and Freundlich
397 isotherm models, and although not an optimal fit, the Langmuir isotherm model
398 described ammonium adsorption better, based on higher *R*² values (0.75-0.91 for
399 commercial oak chars and 0.91 for greenhouse waste 250°C and 600°C). As
400 observed in char PO₄-P sorption, the pseudo-second order model generally had
401 higher *R*² values (**Table 5**) compared to the pseudo-first order and intra-particle
402 diffusion models, although not an optimal fit in many cases.

403 Desorption of NH₄-N after KCl extraction was minimal and this has been observed
404 elsewhere (Clough et al. 2013; Fernando et al. 2005; Saleh et al. 2012). This might
405 have been because NH₄-N was effectively trapped within the biochar pore structure,
406 because the salt solution (KCl) was not effective in extracting adsorbed NH₄-N
407 (Saleh et al. 2012), or due to NH₃-N volatilization especially for high pH biochars
408 (Wang et al. 2015b).

409 **3.6 Possible reaction mechanisms for NH₄⁺ sorption**

410 NH₄-N adsorption was marginally higher in most lower temperature biochars and
411 hydrochars. This general decrease in NH₄-N adsorption with temperature is
412 expected, and Zeng et al. (2013) noted that the absence of aromatic C=O and C=C,
413 -CH₂-, CO and CC functional groups from a high temperature biochar (600 °C) after
414 NH₄-N adsorption suggested that these functional groups reacted with NH₄-N. A
415 positive relationship between biochar acid functional groups and NH₄-N adsorption
416 was observed in Wang et al. (2015a), which corroborated earlier speculations by
417 Zheng et al. (2010) that with increasing pyrolysis temperature, NH₄-N sorption
418 decreased due to loss of biochar polar groups.

419 In terms of nutrient adsorption, it is becoming increasingly apparent that char surface
420 groups may play a more important role than surface area and porosity in both
421 biochars and hydrochars (Bargmann et al. 2014; Spokas et al. 2012). Preliminary
422 studies on municipal waste and presscake biochars pyrolysed in 1% oxygen also
423 showed improved NH₄-N adsorption capacities (data not included). As observed in
424 char CEC, a positive relationship between oxygen content and NH₄-N was observed
425 following solvent-extraction (**Fig 4**). Presscake and commercial oak biochars
426 possessed similar NH₄-N adsorption capacities in spite of very different surface
427 areas (2.5 m² g⁻¹ and 280 m² g⁻¹ respectively), suggesting that physisorption/ion
428 exchange might not be the dominant mechanism by which NH₄-N adsorption
429 occurred. Liang et al. (2006) also noted that high O/C ratios could be responsible for
430 nutrient adsorption since potassium to carbon ratios were at least 0.18 higher at
431 black carbon surfaces than at interior portions.

432 NH₄-N adsorption onto soluble organic matter on char surfaces has also been
433 suggested as a possible process, based on observations of increased NH₄-N

434 adsorption in complex solutions (dairy or swine effluents) compared to simple
435 solutions (ammonium chloride) (Fernando et al. 2005; Sarkhot et al. 2013), although
436 the reverse effect has also been observed, as in Kizito et al. (2015). No clear trends
437 were observed between char organic matter content and $\text{NH}_4\text{-N}$ adsorption capacity
438 in this study.

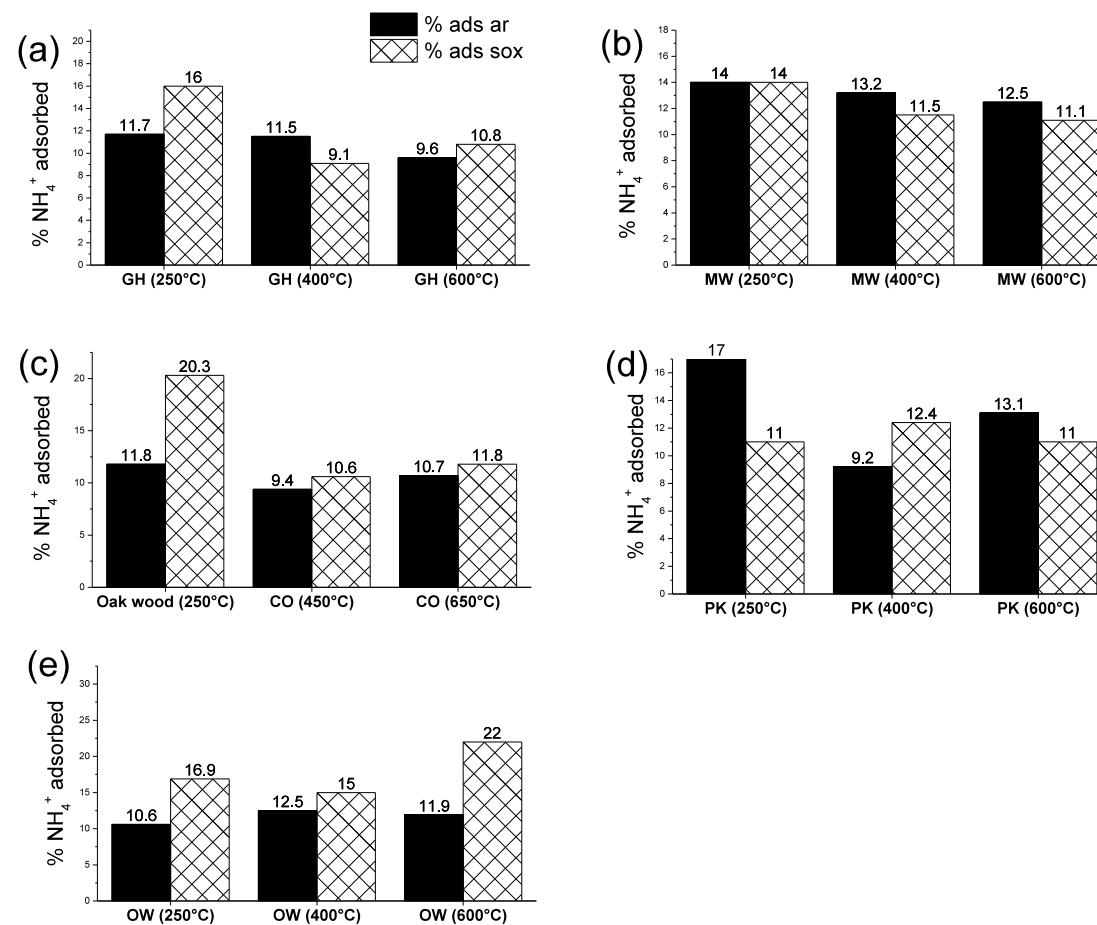


Figure 4. Comparison of $\text{NH}_4\text{-N}$ adsorption capacities of solvent extracted and non-extracted chars showing variable trends; solvent extracted chars denoted by prefix 'S'.

GH: greenhouse waste; MW: municipal waste; CO: commercial oak; OW: oak wood; PK: presscake biochars

440 **Conclusions**

441 This study investigated the phosphate and ammonium adsorption capacities of
442 biochars derived from various waste biomass feed-stocks, comparing key
443 physicochemical properties such as surface area, CEC, ash and mineral content.
444 Solvent extraction improved hydrochar CEC, possibly due to removal of
445 hydrophobic compounds. Conversely, slow pyrolysis biochar CEC generally
446 decreased following solvent extraction.

447 Char $\text{PO}_4\text{-P}$ and $\text{NH}_4\text{-N}$ sorption capacities ranged from about 0-30 mg g^{-1} and
448 105.8-146.4 mg g^{-1} respectively with generally low desorption of both ions. Biochar
449 phosphate adsorption capacity increased with pyrolysis temperature, possibly due to
450 metal ion precipitation reactions between phosphate and char calcium and
451 magnesium. In contrast, a positive relationship between char oxygen functional
452 groups, CEC and $\text{NH}_4\text{-N}$ adsorption suggested that $\text{NH}_4\text{-N}$ adsorption may have
453 occurred mainly via chemical reactions with oxygen-containing functional groups
454 rather than ion-exchange/physisorption. Overall however, in spite of differences in
455 physicochemical properties and processing conditions, there was no great variation
456 in char phosphate and ammonium sorption capacities between the chars.

457

458 **Acknowledgements**

459 This study was funded by The Petroleum Technology Development Fund (PTDF)
460 Nigeria and the FERTIPLUS Consortium (Grant Agreement N°: 289853), co-funded
461 by the European Commission, Directorate General for Research & Innovation, within
462 the 7th Framework Programme of RTD, Theme 2 – Biotechnologies, Agriculture &

463 Food. The views and opinions expressed in this study are purely those of the authors
464 and may not in any circumstances be regarded as stating an official position of the
465 European Commission. The authors also wish to thank the technical staff of the Civil
466 Engineering department and Energy Research Institute, University of Leeds, West
467 Yorkshire, UK.

468

469

470 **References**

- 471 Bargmann, I., Rillig, M.C., Kruse, A., Greef, J.M., Kücke, M., 2014. Effects of hydrochar application on
472 the dynamics of soluble nitrogen in soils and on plant availability. *J. Plant Nutr. Soil Sci.* 177,
473 48–58. doi:10.1002/jpln.201300069
- 474 Barker, J., Zublena, J., Wallis F., 2001. *Animal and Poultry Manure Production and*
475 *Characterization*, North Carolina State University Cooperative Extension.
476 <https://www.bae.ncsu.edu/topic/animal-waste-mgmt/program/land-ap/barker/a&pmp&c/content.htm>
- 477 Battistoni, P., Carniani, E., Fratesi, V., Balboni, P., Tornabuoni, P., 2006. Chemical-Physical
478 Pretreatment of Phosphogypsum Leachate. *Ind. Eng. Chem. Res.* 45, 3237–3242.
479 doi:10.1021/ie051252h
- 480 Biederman, L.A., Harpole, W.S., 2013. Biochar and its effects on plant productivity and nutrient
481 cycling: a meta-analysis. *GCB Bioenergy* 5, 202–214. doi:10.1111/gcbb.12037
- 482 Boehm, H.P., 1994. Some aspects of the surface chemistry of carbon blacks and other carbons.
483 *Carbon N. Y.* 32, 759–769. doi:10.1016/0008-6223(94)90031-0
- 484 Borchard, N., Wolf, A., Laabs, V., Aeckersberg, R., Scherer, H., Moellerand, A., Amelung, W., 2012.
485 Physical activation of biochar and its meaning for soil fertility and nutrient leaching- A
486 greenhouse experiment, *Soil Use Manage.* 28:177-184. doi: 10.1111/j.14752743.2012.00407.x
- 487 Bott, C.B., Brummer, J., Koon, J., 2003. Physical-chemical pretreatment of process wastewater
488 from a phosphorus plant for discharge to a POTW. In: Bowers, A., and W. Eckenfelder. 2003.
489 *Industrial wastewater and Best Available Treatment technologies: Performance, reliability, and*
490 *economics*, DEStech Publications Inc.
- 491 Brewer, C.E., 2012. *Biochar Characterisation and Engineering*. <http://lib.dr.iastate.edu/etd/12284/>
- 492 Cai, T., Park, S.Y., Li, Y., 2013. Nutrient recovery from wastewater streams by microalgae: Status and
493 prospects. *Renew. Sustain. Energy Rev.* 19, 360–369. doi:10.1016/j.rser.2012.11.030
- 494 Chen, B., Chen, Z., Lv, S., 2011. A novel magnetic biochar efficiently sorbs organic pollutants and
495 phosphate. *Bioresour. Technol.* 102, 716–23. doi:10.1016/j.biortech.2010.08.067
- 496 Clough, T., Condon, L., Kammann, C., Müller, C., 2013. A Review of Biochar and Soil Nitrogen
497 Dynamics. *Agronomy* 3, 275–293. doi:10.3390/agronomy3020275
- 498 Collison, M., Collison, L., Sakrabani, R., Tofield, B., Wallage, Z., 2009. *Biochar and Carbon*
499 *Sequestration: A Regional Perspective: A Report Prepared for East of England Development*
500 *Agency (EEDA)*.
501 [https://www.uea.ac.uk/polopoly_fs/1.118134!LCIC%20EEDA%20BIOCHAR%20REVIEW%202004-](https://www.uea.ac.uk/polopoly_fs/1.118134!LCIC%20EEDA%20BIOCHAR%20REVIEW%202004-09.pdf)
502 [09.pdf](https://www.uea.ac.uk/polopoly_fs/1.118134!LCIC%20EEDA%20BIOCHAR%20REVIEW%202004-09.pdf)
- 503 Fernando, W.A., Xia, K., Rice, C.W., 2005. Sorption and Desorption of Ammonium from Liquid Swine
504 Waste in Soils. *Soil Sci. Soc. Am. J.* 69, 1057. doi:10.2136/sssaj2004.0268
- 505 Gaskin, J., Steiner, C., Harris, K., Das, K., Bibens, B., 2008. Effect of low-temperature
506 pyrolysis conditions on biochar for agricultural use, *T. Am. Soc. Agr. Biol. Eng.* 51, 2061-2069.

507 Glaser, B., Lehmann, J., Zech, W., 2002. Ameliorating physical and chemical properties of highly
508 weathered soils in the tropics with charcoal - a review. *Biol. Fertil. Soils* 35, 219–230.
509 doi:10.1007/s00374-002-0466-4

510 Grzmil, B., Wronkowski, J., 2006. Removal of phosphates and fluorides from industrial wastewater.
511 *Desalination* 189, 261–268. doi:10.1016/j.desal.2005.07.008

512 Heilmann, S.M., Jader, L.R., Harned, L.A., Sadowsky, M.J., Schendel, F.J., Lefebvre, P.A., von Keitz,
513 M.G., Valentas, K.J., 2011. Hydrothermal carbonization of microalgae II. Fatty acid, char, and
514 algal nutrient products. *Appl. Energy* 88, 3286–3290. doi:10.1016/j.apenergy.2010.12.041

515 Ho, Y., 2004. Selection of optimum sorption isotherm. *Carbon*. 42, 2113-2130.
516 doi:10.1016/j.carbon.2004.03.019

517 International Biochar Initiative, 2014. Standardized product definition and product testing
518 guidelines for biochar that is used in soil. [http://www.biochar-](http://www.biochar-international.org/sites/default/files/IBI_Biochar_Standards_V2%200_final_2014.pdf)
519 [international.org/sites/default/files/IBI_Biochar_Standards_V2%200_final_2014.pdf](http://www.biochar-international.org/sites/default/files/IBI_Biochar_Standards_V2%200_final_2014.pdf)

520 Kastner, J.R., Miller, J., Das, K., 2009. Pyrolysis conditions and ozone oxidation effects on ammonia
521 adsorption in biomass generated chars. *J. Haz. Mat.* 164, 1420-1427.
522 doi:10.1016/j.jhazmat.2008.09.051

523 Kizito, S., Wu, S., Kirui, W., Lei, M., Lu, Q., Bah, H., Dong, R., 2015. Evaluation of slow pyrolyzed
524 wood and rice husks biochar for adsorption of ammonium nitrogen from piggery manure
525 anaerobic digestate slurry, *Sci. Total Environ.* 505, 102-112. doi:10.1016/j.scitotenv.2014.09.096

526 Krishnan, K.A., Haridas, A., 2008. Removal of phosphate from aqueous solutions and sewage using
527 natural and surface modified coir pith. *J. Hazard. Mater.* 152, 527–35.
528 doi:10.1016/j.jhazmat.2007.07.015

529 Kumar, K.V., Sivanesan, S., 2007. Sorption isotherms for safranin onto rice husk: Comparison of
530 linear and non-linear methods. *Dyes Pigments*. 72, 130-133. doi:10.1016/j.dyepig.2005.07.020

531 Laird, D., Fleming, P., Wang, B., Horton, R., Karlen, D., 2010a. Biochar impact on nutrient leaching
532 from a Midwestern agricultural soil. *Geoderma* 158, 436–442.
533 doi:10.1016/j.geoderma.2010.05.012

534 Laird, D.A., Fleming, P., Davis, D.D., Horton, R., Wang, B., Karlen, D.L., 2010b. Impact of biochar
535 amendments on the quality of a typical Midwestern agricultural soil. *Geoderma* 158, 443–449.
536 doi:10.1016/j.geoderma.2010.05.013

537 Lehmann, J., 2007. Bio-energy in the black. *Front. Ecol. Environ.* 5, 381–387. doi:10.1890/1540-
538 9295(2007)5[381:BITB]2.0.CO;2

539 Liang, B., Lehmann, J., Solomon, D., Kinyangi, J., Grossman, J., O'Neill, B., Skjemstad, J.O., Thies,
540 J., Luizão, F.J., Petersen, J., Neves, E.G., 2006. Black Carbon Increases Cation Exchange
541 Capacity in Soils. *Soil Sci. Soc. Am. J.* 70, 1719. doi:10.2136/sssaj2005.0383

542 Limousin, G., Gaudet, J.-P., Charlet, L., Szenknect, S., Barthès, V., Krimissa, M., 2007. Sorption
543 isotherms: A review on physical bases, modeling and measurement. *Appl. Geochemistry* 22,
544 249–275. doi:10.1016/j.apgeochem.2006.09.010

545 Liu, J.C., 2009. Recovery of phosphate and ammonium as struvite from semiconductor wastewater.
546 *Sep. Purif. Technol.* 64, 368–373. doi:10.1016/j.seppur.2008.10.040

547 Mukherjee, A., Zimmerman, A.R., 2013. Organic carbon and nutrient release from a range of
548 laboratory-produced biochars and biochar–soil mixtures. *Geoderma* 193-194, 122–130.
549 doi:10.1016/j.geoderma.2012.10.002

550 Poerschmann, J., Weiner, B., Koehler, R., Kopinke, F.-D., 2015. Organic breakdown products
551 resulting from hydrothermal carbonization of brewer's spent grain. *Chemosphere* 131, 71–7.
552 doi:10.1016/j.chemosphere.2015.02.057

553 Rittmann, B.E., Mayer, B., Westerhoff, P., Edwards, M., 2011. Capturing the lost phosphorus.
554 *Chemosphere* 84, 846–853. doi:10.1016/j.chemosphere.2011.02.001

555 Saleh, M.E., Mahmoud, A., Rashad, M., 2012. Peanut biochar as a stable adsorbent for removing
556 NH₄-N from wastewater: A preliminary study, *Adv. Environ. Biol.* 6, 2170-2176.
557 doi:10.3390/agronomy3020275

558 Sakadevan, K., Bavor, H.J., 1998. Phosphate adsorption characteristics of soils, slags and zeolite to
559 be used as substrates in constructed wetland systems. *Water Res.* 32, 393–399.
560 doi:10.1016/S0043-1354(97)00271-6

561 Sarkhot, D. V, Berhe, A.A., Ghezzehei, T.A.,. Impact of biochar enriched with dairy manure effluent on
562 carbon and nitrogen dynamics. *J. Environ. Qual.* 41, 1107–14. doi:10.2134/jeq2011.0123

563 Silber, A., Levkovitch, I., Graber, E.R., 2010. pH-dependent mineral release and surface properties of
564 cornstraw biochar: agronomic implications. *Environ. Sci. Technol.* 44, 9318–23.
565 doi:10.1021/es101283d

566 Song, Y.-H., Qiu, G.-L., Yuan, P., Cui, X.-Y., Peng, J.-F., Zeng, P., Duan, L., Xiang, L.-C., Qian, F.,
567 2011. Nutrients removal and recovery from anaerobically digested swine wastewater by struvite
568 crystallization without chemical additions. *J. Hazard. Mater.* 190, 140–9.
569 doi:10.1016/j.jhazmat.2011.03.015

570 Spokas, K.A., Novak, J.M., Venterea, R.T., 2011. Biochar's role as an alternative N-fertilizer:
571 ammonia capture. *Plant Soil* 350, 35–42. doi:10.1007/s11104-011-0930-8

572 USEPA, 2002. Onsite wastewater treatment systems manual.
573 http://water.epa.gov/aboutow/owm/upload/2004_07_07_septics_septic_2002_osdm_all.pdf

574 Uzoma, K.C., Inoue, M., Andry, H., Fujimaki, H., Zahoor, A., Nishihara, E., 2011. Effect of cow
575 manure biochar on maize productivity under sandy soil condition. *Soil Use Manag.* 27, 205–212.
576 doi:10.1111/j.1475-2743.2011.00340.x

577 Vasanth Kumar, K., Sivanesan, S., 2007. Sorption isotherm for safranin onto rice husk: Comparison
578 of linear and non-linear methods. *Dye. Pigment.* 72, 130–133. doi:10.1016/j.dyepig.2005.07.020

579 Wang, Z., Nie, E., Li, J., Yang, M., Zhao, Y., Luo, X., Zheng, Z., 2011. Equilibrium and kinetics of
580 adsorption of phosphate onto iron-doped activated carbon. *Environ. Sci. Pollut. Res. Int.* 19,
581 2908–17. doi:10.1007/s11356-012-0799-y

582 Wang, Z., Guo, H., Shen, F., Yang, G., Zhang, Y., Zeng, Y., Wang, L., Xiao, H., Deng, S., 2015a.
583 Biochar produced from oak sawdust by Lanthanum (La)-involved pyrolysis for adsorption of
584 ammonium (NH₄⁺), nitrate (NO₃⁻), and phosphate (PO₄³⁻). *Chemosphere* 119, 646–653.
585 doi:10.1016/j.chemosphere.2014.07.084

586 Wang, B., Lehmann, J., Hanley, K., Hestrin, R., Enders, A., 2015b. Adsorption and desorption of
587 ammonium by maple wood biochar as a function of oxidation and pH. *Chemosphere* 138, 120–
588 126. doi:10.1016/j.chemosphere.2015.05.062

589 Warner, S.A., 1977. Cation exchange properties of forest litter as influenced by vegetation type and
590 Decomposition. <http://andrewsforest.oregonstate.edu/pubs/pdf/pub533.pdf>

591 Xu, G., Sun, J., Shao, H., Chang, S.X., 2014. Biochar had effects on phosphorus sorption and
592 desorption in three soils with differing acidity. *Ecol. Eng.* 62, 54–60.
593 doi:10.1016/j.ecoleng.2013.10.027

594 Xue, Y., Hou, H., Zhu, S., 2009. Characteristics and mechanisms of phosphate adsorption onto basic
595 oxygen furnace slag. *J. Hazard. Mater.* 162, 973–80. doi:10.1016/j.jhazmat.2008.05.131

596 Xue, Y., Gao, B., Yao, Y., Inyang, M., Zhang, M., Zimmerman, A.R., Ro, K.S., 2012. Hydrogen
597 peroxide modification enhances the ability of biochar (hydrochar) produced from hydrothermal
598 carbonization of peanut hull to remove aqueous heavy metals: Batch and column tests. *Chem.*
599 *Eng. J.* 200-202, 673–680. doi:10.1016/j.cej.2012.06.116

600 Yamato, M., Okimori, Y., Wibowo, I.F., Anshori, S., Ogawa, M., 2006. Effects of the application of
601 charred bark of *Acacia mangium* on the yield of maize, cowpea and peanut, and soil chemical
602 properties in South Sumatra, Indonesia. *Soil Sci. Plant Nutr.* 52, 489–495. doi:10.1111/j.1747-
603 0765.2006.00065.x

604 Yao, Y., Gao, B., Chen, J., Yang, L., 2013. Engineered biochar reclaiming phosphate from aqueous
605 solutions: mechanisms and potential application as a slow-release fertilizer. *Environ. Sci.*
606 *Technol.* 47, 8700–8. doi:10.1021/es4012977

607 Yao, Y., Gao, B., Inyang, M., Zimmerman, A.R., Cao, X., Pullammanappallil, P., Yang, L., 2011.
608 Biochar derived from anaerobically digested sugar beet tailings: characterization and phosphate
609 removal potential. *Bioresour. Technol.* 102, 6273–8. doi:10.1016/j.biortech.2011.03.006

610 Ye, Y., Hou, H., Zhu, S., 2006. Characteristics and mechanisms of phosphate adsorption onto basic
611 oxygen furnace slag, *J. Hazard. Mater.* 162, 973–980. doi: 10.1016/j.jhazmat.2008.05.131

612 Ye, Z.L., Chen, S.H., Wang, S.M., Lin, L.F., Yan, Y.J., Zhang, Z.J., Chen, J.S., 2010. Phosphorus
613 recovery from synthetic swine wastewater by chemical precipitation using response surface
614 methodology. *J. Hazard. Mater.* 176, 1083–8. doi:10.1016/j.jhazmat.2009.10.129

615 Yuan, J.-H., Xu, R.-K., Zhang, H., 2011. The forms of alkalis in the biochar produced from crop
616 residues at different temperatures. *Bioresour. Technol.* 102, 3488–97.
617 doi:10.1016/j.biortech.2010.11.018

618 Zeng, Z., Zhang, S., Li, T., Zhao, F., He, Z., Zhao, H., Yang, X., Wang, H., Zhao, J., Rafiq, M.T., 2013.
619 Sorption of ammonium and phosphate from aqueous solution by biochar derived from
620 phytoremediation plants. *J. Zhejiang Univ. Sci. B* 14, 1152–61. doi:10.1631/jzus.B1300102

621 Zhang, M., Gao, B., Yao, Y., Xue, Y., Inyang, M., 2012. Synthesis of porous MgO-biochar
622 nanocomposites for removal of phosphate and nitrate from aqueous solutions. Chem. Eng. J.
623 210, 26–32. doi:10.1016/j.cej.2012.08.052
624 Zhao, L., Cao, X., Mašek, O., Zimmerman, A., 2013. Heterogeneity of biochar properties as a function
625 of feedstock sources and production temperatures. J. Hazard. Mater. 256-257, 1–9.
626 doi:10.1016/j.jhazmat.2013.04.015
627 Zheng, W., Sharma, B.K., Rajagopalan, N., 2010. Using Biochar as a Soil Amendment for
628 Sustainable Agriculture. <https://www.ideals.illinois.edu/handle/2142/25503>
629
630
631
632
633